Molecular Vision 2019; 25:890-901 <http://www.molvis.org/molvis/v25/890>
Received 30 June 2018 | Accepted 30 December 2019 | Published 31 December 2019

Reduced expression of the *nob8* gene does not normalize the distribution or function of mGluR6 in the mouse retina

Junzo Kinoshita,[1] Nazarul Hasan,[2] Brent A. Bell,[1] Neal S. Peachey[1,3,4]

[1]Cole Eye Institute, Cleveland Clinic, Cleveland, OH; [2]Department of Biochemistry & Molecular Genetics, University of Louisville, Louisville, KY; [3]Research Service, Louis Stokes Cleveland VA Medical Center, Cleveland, OH; [4]Department of Ophthalmology, Cleveland Clinic Lerner College of Medicine of Case Western Reserve University, Cleveland, OH

Purpose: The *Grm6*^{nob8} mouse carries a missense mutation in the *Grm6* gene (p.Met66Leu), and exhibits a reduced b-wave of the electroretinogram (ERG), abnormal localization of metabotropic glutamate receptor 6 (mGluR6) to the depolarizing bipolar cell (DBC) soma, and a reduced level of mGluR6 at the DBC dendritic tips. Although the underlying mechanism remains unknown, one possible explanation is that DBCs cannot efficiently traffic the mutant mGluR6. In that scenario, reducing the total amount of mutant mGluR6 protein might normalize localization, and thus, improve the ERG phenotype as well. The second purpose of this study was to determine whether the abnormal cellular distribution of mutant mGluR6 in *Grm6*^{nob8} retinas might induce late onset DBC degeneration.
Methods: We crossed *Grm6*^{nob8} animals with *Grm6*^{nob3} mice, which carry a null mutation in *Grm6*, to generate *Grm6*$^{nob3/nob8}$ compound heterozygotes. We used western blotting to measure the total mGluR6 content, and immunohistochemistry to document mGluR6 localization within DBCs. In addition, we examined outer retinal function with ERG and retinal architecture in vivo with spectral domain optical coherence tomography (SD-OCT).
Results: The retinal content of mGluR6 was reduced in the retinas of the *Grm6*$^{nob3/nob8}$ compound heterozygotes compared to the *Grm6*^{nob8} homozygotes. The cellular distribution of mGluR6 in the *Grm6*$^{nob3/nob8}$ compound heterozygotes matched that of the *Grm6*^{nob8} homozygotes, with extensive expression throughout the DBC cell body and limited expression at the DBC dendritic tips. The dark-adapted ERG b-waves of the *Grm6*$^{nob3/nob8}$ mice were reduced in comparison to those of the *Grm6*^{nob8} homozygotes at postnatal day 21 and 28. The overall ERG waveforms obtained from 4- through 68-week old *Grm6*^{nob8} mice were in general agreement for dark- and light-adapted conditions. The maximum response and sensitivity of the dark-adapted ERG b-wave did not change statistically significantly with age. SD-OCT revealed the maintained laminar structure of the retina, including a clear inner nuclear layer (INL) at each age examined (from 11 to 57 weeks old), although the INL in the mice older than 39 weeks of age was somewhat thinner than that seen at 11 weeks.
Conclusions: Mislocalization of mutant mGluR6 is not normalized by reducing the total mGluR6. Mislocalized mutant mGluR6 does not trigger substantial loss of DBCs.

The signal transduction cascade of depolarizing bipolar cells (DBCs) is initiated when a light-induced reduction in glutamate release from photoreceptor terminals is sensed by the metabotropic glutamate receptor 6 (mGluR6) [1,2]. DBC activity underlies the b-wave component of the electroretinogram (ERG) [3-7], and the b-wave is missing in humans carrying mutations in *GRM6* (OMIM 604096) [8,9], and in mouse models lacking mGluR6 due to null mutations in *Grm6* [10-13].

We recently reported the *Grm6*^{nob8} mutant mouse model in which the ERG b-wave is reduced but is not eliminated [14]. The mouse carries a missense mutation, p.Met66Leu. Immunohistochemistry documented abnormal distribution of mGluR6, with a substantial fraction retained within the DBC soma and abnormally low levels of mGluR6 at the DBC dendritic tips. In the *Grm6*^{nob8} model, mutant mGluR6 was abnormally glycosylated, a state that has been shown to result in abnormal trafficking of other G-protein coupled receptors [15-17].

In the present report, we follow up on the observation in the mouse model mentioned above in two respects. To determine whether reducing levels of mutant mGluR6 might normalize localization within *Grm6*^{nob8} DBCs, we genetically reduced the amount of mGluR6 by crossing the *Grm6*^{nob8} mutant with a Grm6 null model (*Grm6*^{nob3}). Although we are unaware of a comparable approach, we note that mislocalized mutant proteins are associated with neuronal degeneration in other systems [e.g., 18,19]. Given the relevance of *Grm6* mutant mice to the human condition complete congenital stationary night blindness (cCSNB) [14] and the identification of human mutations near the *nob8* locus [20], we examined the retinal structure and function in *Grm6*^{nob8} mice at ages up to 1 year old.

Correspondence to: Junzo Kinoshita, 1-16-13, Kitakasai, Edogawa, Tokyo 134-8630, Japan, Phone: +81-3-3680-0151; FAX: +81-3-5696-8335; email: kinoshita.junzo.dy@daiichisankyo.co.jp

METHODS

Mice: Mice were obtained from the Jackson Laboratory (Bar Harbor, ME). The lines used were CBA/CaJ that are homozygous for the *Grm6*^{nob8} allele (stock #000654; hereafter *Grm6*^{nob8}), C57BL/6J (stock #000664), and B6.B10(D2)-*Grm6*^{nob3}/BOC mice that are homozygous for a null mutation in *Grm6* [12]; hereafter, *Grm6*^{nob3}. In addition to these homozygous lines, we crossed *Grm6*^{nob8} and *Grm6*^{nob3} mice to generate *Grm6*$^{nob3/nob8}$ compound heterozygotes. Mice were housed conventionally, in microisolator cages with free access to food and water. All procedures involving live animals were approved by the Cleveland Clinic Institutional Animal Care and Use Committee, and were conducted in accordance with the ARVO Statement for the Use of Animals in Ophthalmic and Vision Research.

Western blotting: Mouse retinas were isolated and homogenized in lysis buffer (1% Nonidet P40, 2 mM EDTA, and 20 mM HEPES, pH 7.4, supplemented with protease inhibitor cocktail (P8340, Sigma-Aldrich, St. Louis, MO), and lysed further by rotating at 4 °C for 45 min. Homogenates were cleared by centrifugation at 17,000 ×*g* for 20 min at 4 °C. Protein samples were separated with sodium dodecyl sulfate–polyacrylamide gel electrophoresis (SDS–PAGE) and transferred to polyvinylidene fluoride (PVDF) membranes, and immunoblotting was performed as described previously [21]. Protein bands were visualized by scanning the membranes in an Odyssey Infrared Imaging System (LI-COR, Lincoln, NE) using 700 nm and 800 nm channels. Band densities were quantified using Image Studio Version 5.0 software (LI-COR).

Immunohistochemistry: At 4 weeks, the mice were euthanized with carbon dioxide inhalation, and the eyes were enucleated. Dissected retinas were fixed for 20 min by immersion in 4% (w/v) paraformaldehyde in 0.1 M phosphate buffer (PB) with a pH 7.4, then washed in PB, cryoprotected through a graded sucrose series (5%,10%, 15%, and 20% in PB), and frozen in OCT (Sakura Finetek, Torrance, CA):20% sucrose (2:1) [22]. A cryostat was used to cut 18-µm sections, which were then mounted on Super-Frost glass slides (Thermo Fisher Scientific, Waltham, MA), air-dried, and stored at −80 °C.

After acclimating to room temperature, the sections were washed for 5 min in PBS (137 mM NaCl, 2.7 mM KCl, 10 mM Na_2HPO_4, 1.8 mM KH_2PO_4, pH 7.4), then another 5 min in PBX (PBS containing 0.5% (v/v) Triton X-100), and then incubated for 1 h in blocking solution (PBX containing 5% (v/v) normal donkey serum). The retinal sections were incubated in primary antibodies diluted in blocking solution, at room temperature overnight. The antibody against mouse mGluR6 amino acids 853–871 (KKTSTMAAPPKSENSEDAK) was generated in sheep [23]. Anti-PKCα antibody was used at 1:1,000 dilution (Sigma, P4334). After incubation with the primary antibody, the sections were washed with three 10-min cycles of PBX and one 10-min cycle of PBS. The sections were then incubated at room temperature for 1 h with fluorescently labeled secondary antibodies (1:1,000 in blocking solution). The secondary antibodies were Alexa Fluor 488 donkey anti-sheep and Alexa Fluor 546 donkey anti-rabbit (Invitrogen, Carlsbad, CA). The slides were then washed three times in PBX and coverslipped with Vectashield Mounting Media (Vector Laboratories, Burlingame, CA). The sections were imaged on a confocal microscope (Olympus FV1000, Center Valley, PA), using a 60X oil objective (1.45 NA). Images shown here are maximum projections of confocal stacks, after adjustment for contrast and brightness with Fluoview software.

Electroretinography: Mice were dark-adapted overnight, anesthetized (ketamine: 80 mg/kg; xylazine: 16 mg/kg), and administered eye drops for pupil dilation (1% tropicamide; 2.5% phenylephrine HCl; 1% cyclopentolate HCl) and to anesthetize the corneal surface (1% proparacaine HCl). Needle electrodes were placed in the cheek (reference) and tail (ground). ERGs were recorded using a stainless steel electrode wetted with 1% carboxymethylcellulose.

Strobe flash stimuli were presented to the dark-adapted eye, and after a minimum of 5 min of light adaptation using background illumination at 20 cd/m^2. Stimuli ranged from −3.6 to 2.1 log cd s/m^2. Responses were amplified (0.03–1,000 Hz), averaged, and stored using an LKC (Gaithersburg, MD) UTAS E-3000 signal averaging system.

The amplitude of the dark-adapted ERG a-wave was measured from the prestimulus baseline to 8 ms after the flash onset. The amplitude of the b-wave was measured from the a-wave trough to the positive peak, or from the baseline to the positive peak for stimulus conditions that did not evoke an a-wave. The amplitude of the light-adapted ERG b-wave was measured from the initial negative trough to 40 ms after the flash onset.

The stimulus-response function of the dark-adapted b-wave was fitted with a hyperbolic equation of the following form [24]:

$$R / R_{max} = L^n / (L^n + K^n).$$

In this equation, R is the b-wave amplitude, R_{max} is the maximum b-wave amplitude, L is the flash luminance (log cd s/m^2), n is a dimensionless slope parameter, and K is the flash energy that elicits an amplitude of half R_{max} (half-saturation coefficient). This model yielded values for two parameters (i.e., R_{max} and K). *Grm6*$^{nob3/nob8}$ and *Grm6*^{nob8} mice were tested

at postnatal day (P) 15, P21, and P28. The *Grm6*^{nob8} mice were also tested at 9, 28, 48, and 68 weeks of age.

In vivo retinal imaging: Procedures for animal preparation, imaging, and recovery have been published [25,26]. Briefly, a Bioptigen (Durham, NC) model SDOIS SD-OCT system was used for spectral domain optical coherence tomography (SD-OCT) imaging. B-scans were made through the optic nerve head at 1,000 A-scans/B-scan × 30 frames. B-scan images had dimensions of 0.4 mm (depth) by approximately 1.6 mm (width), and were exported to ImageJ, coregistered, and averaged using StackReg/TurboReg/Plugins [27]. Using SD-OCT images taken across the horizontal and vertical meridians from each mouse, the thickness of the inner nuclear layer (INL) was measured at a point midway between the optic nerve head and the edge of the image. The *Grm6*^{nob8} mice were imaged at three ages (11, 39, and 57 weeks old).

RESULTS

Impact of reduced levels of mutant mGluR6: The *Grm6*^{nob8} retina is characterized by a selective reduction in the amplitude of the ERG b-wave and mislocalization of mGluR6 to the cell body of DBCs, as opposed to its normal restriction to the DBC dendritic tips [14]. To determine whether either of these abnormalities might be ameliorated by reducing the total amount of mutant mGluR6 protein, we compared these features in *Grm6*^{nob8} homozygotes and *Grm6*$^{nob3/nob8}$ compound heterozygotes. These mice differ with respect to the total content of mGluR6, with retinas of *Grm6*$^{nob3/nob8}$ compound heterozygotes having approximately half compared to *Grm6*^{nob8} homozygotes (Figure 1A,B).

The mGluR6 expression was observed only in the DBC dendritic tips of the control mice (Figure 2A,C), with no overlap with PKCα labeling in the DBC soma (Figure 2B,C). In the *Grm6*^{nob8} homozygotes, mGluR6 expression was reduced (Figure 1D) and colocalized with PKCα in DBC soma (Figure 2E,F). The distribution of mGluR6 in the *Grm6*$^{nob3/nob8}$ compound heterozygotes (Figure 2G–I) matched that of the *Grm6*^{nob8} homozygotes with extensive expression throughout the cell body and limited expression at the DBC dendritic tips. This result indicates that the mislocalization of mGluR6 was not corrected when only a single *Grm6*^{nob8} allele was expressed, resulting in a reduction in the total amount of mutant mGluR6 (Figure 1A,B).

When the *Grm6*$^{nob3/nob8}$ compound heterozygotes were examined with ERG, the results complemented those obtained with immunohistochemistry. In Figure 3A, the ERG phenotypes of representative *Grm6*^{nob8} and *Grm6*$^{nob3/nob8}$ mice are compared at P28, along with a reference control mouse at the same age. The dark-adapted a-waves in the *Grm6*$^{nob3/nob8}$ mice showed amplitudes and kinetics that were comparable to those of the *Grm6*^{nob8} mice (Figure 3A,B; $p>0.05$). In contrast, the dark-adapted b-waves of the *Grm6*$^{nob3/nob8}$ mice were statistically significantly smaller than those in the *Grm6*^{nob8} mice (Figure 3A,B; $p<0.01$), consistent with these mice expressing a single *Grm6*^{nob8} allele. The small b-wave and oscillatory potentials present in the dark-adapted ERGs of the *Grm6*$^{nob3/nob8}$ mice are, however, clearly larger than those reported for the *Grm6*^{nob3} homozygotes [12,13]. There was no statistically significant difference in the amplitude of the light-adapted b-waves obtained from the *Grm6*^{nob8} and *Grm6*$^{nob3/nob8}$ mice (Figure 3C,D; $p>0.05$).

We also used ERG to examine mice at younger ages. Figure 4 presents representative ERGs obtained from *Grm6*^{nob8} homozygotes (black) and *Grm6*$^{nob3/nob8}$ compound heterozygotes (red) at P15 and P21. At P21, a clear albeit reduced b-wave was present in all animals, with a greater reduction observed in the *Grm6*$^{nob3/nob8}$ compound heterozygotes compared to the *Grm6*^{nob8} homozygotes. We did not detect a b-wave in either the *Grm6*$^{nob3/nob8}$ compound heterozygotes or the *Grm6*^{nob8} homozygotes at P15, an age when the retina is still developing, and the ERG has not taken on an adult configuration [28].

Changes in the older Grm6^{nob8} *retina:* To examine whether the *Grm6*^{nob8} phenotype might change with age, we examined mice at different ages. The overall waveforms of the ERGs obtained from 4- and 68-week old *Grm6*^{nob8} mice were in good general agreement for dark- and light-adapted conditions (Figure 5A,C). Figures 5B,D present summary luminance-response functions for ERG components obtained from mice at 4, 9, 28, 48, and 68 weeks of age. These data are not indicative of a progressive age-related change in the ERG amplitude. We further analyzed the dark-adapted b-wave luminance-response functions using the Naka-Rushton equation, which derives two parameters: the maximum response (R_{max}) and the sensitivity (K). The R_{max} values appeared to decrease slightly with age, which is in good agreement with a previous report showing a slight decrease in the ERG amplitude with age in wild-type mice [29]. When the values seen at the youngest age (4 weeks old) were compared to the later time points, the difference was not statistically significant (Figure 5E; $p>0.05$). The sensitivity parameter K trended upward with age (Figure 5F). When the K values of the 4-week-old mice were compared to those obtained from the two oldest ages, there was no statistically significant difference ($p>0.05$). Together, these results indicate that retinal dysfunction in *Grm6*^{nob8} mice is not progressive.

In Figure 6A, the SD-OCT images taken across the horizontal meridian from *Grm6*^{nob8} mice at 11, 39, and 57 weeks

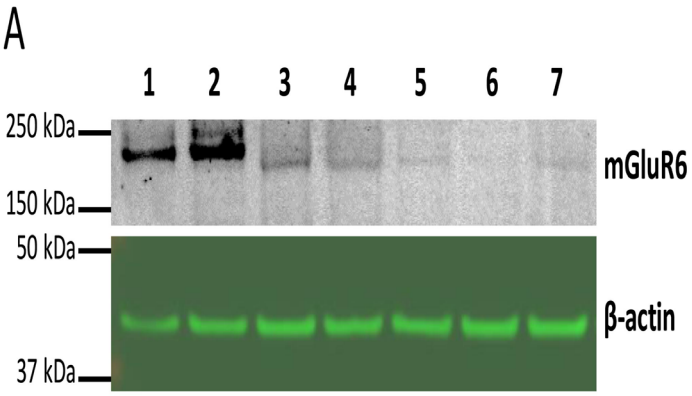

Lane 1,2: WT retinas
Lane 3,4: nob8/nob8 retinas
Lane 5,7: nob3/nob8 retinas
Lane 6: nob3/nob3 retina

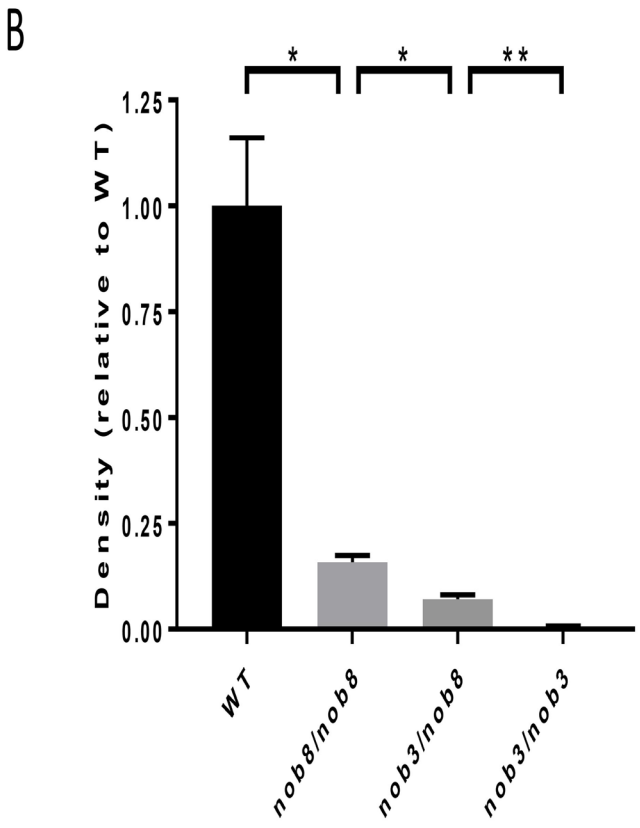

Figure 1. Western blotting analysis of mGluR6 content in WT and *Grm6* mutants. **A**: Western blots for mGluR6 in wild-type (WT; lanes 1 and 2), *Grm6*^{nob8} homozygotes (lanes 3 and 4), *Grm6*$^{nob3/nob8}$ compound heterozygotes (lanes 5 and 7), and a *Grm6*^{nob3} homozygote (lane 6). **B**: Densitometric analysis of western blots, demonstrating that mGluR6 levels are dramatically reduced in all *Grm6* mutants, and that mGlur6 levels of *Grm6*$^{nob3/nob8}$ compound heterozygotes are reduced to approximately half of the levels seen in *Grm6*^{nob8} homozygotes. Each bar indicates average +/− standard error of three samples. Statistically significant differences were detected between groups with Aspin-Welch's *t* test (*p<0.05, **p<0.01).

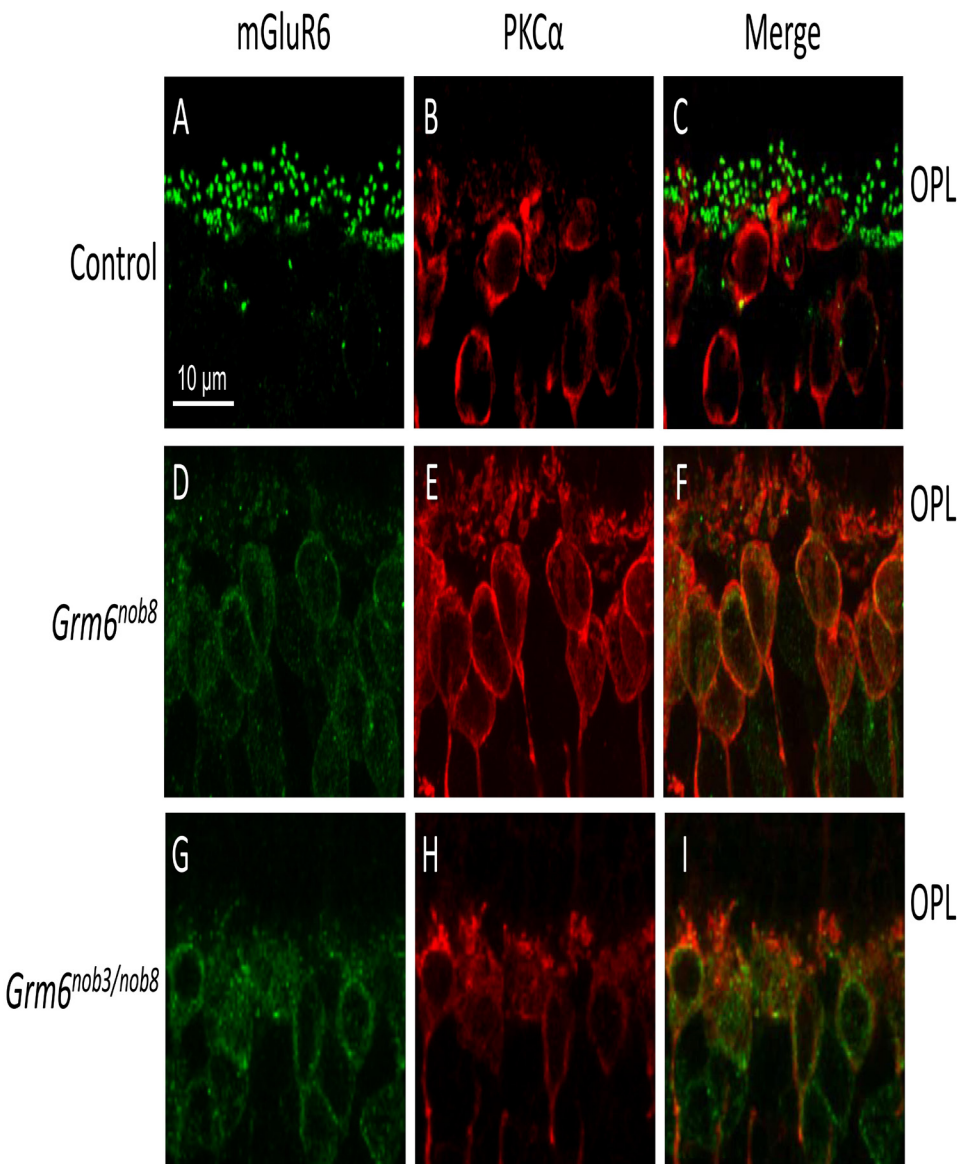

Figure 2. Cellular localization of mGluR6 and PKCα in retinas from the mice at 4 weeks of age. In contrast to the control retinas (**A**–**C**), the *Grm6*$^{nob3/nob8}$ retinas (**G**–**I**) exhibited a similar mGluR6 distribution pattern to that of the *Grm6*^{nob8} retinas (**D**–**F**). Scale bars: 10 µm. OPL, outer plexiform layer.

of age are compared. At each age examined, a clear INL, housing bipolar cell nuclei, was seen in the *Grm6*^{nob8} mice. Although the INL thickness in the mice at 39 weeks or older was thinner than that at 11 weeks old (Figure 6B), the laminar structure of the retina was maintained until the oldest age was tested.

DISCUSSION

Unlike other *Grm6* mouse models, where the retina lacks mGluR6 protein due to a null mutation [10-13], mGluR6 is detected in the *Grm6*^{nob8} retina [14]. The distribution of the mutant protein differs from that of the wild type. First, mGluR6 is clearly seen in the DBC soma. Second, the amount of protein that is successfully trafficked to the DBC dendritic tips is reduced. In agreement with mislocalized mGluR6, the ERG b-wave is reduced in *Grm6*^{nob8} mice, and retinal ganglion cell function is also impaired [14]. The mislocalization of mutant mGluR6 could be related to abnormal protein folding and trafficking mechanisms, secondary to the abnormal glycosylation of mGluR6 noted in the *Grm6*^{nob8} retina [14].

We hypothesized that reducing the total amount of mutant mGluR6 protein might improve the amount of mGluR6 that is successfully delivered to the DBC dendritic tips. Previous studies demonstrated that a single copy of WT *Grm6* is sufficient to support normal DBC function [30], and therapeutic strategies (such as hammerhead ribozymes) exist to reduce

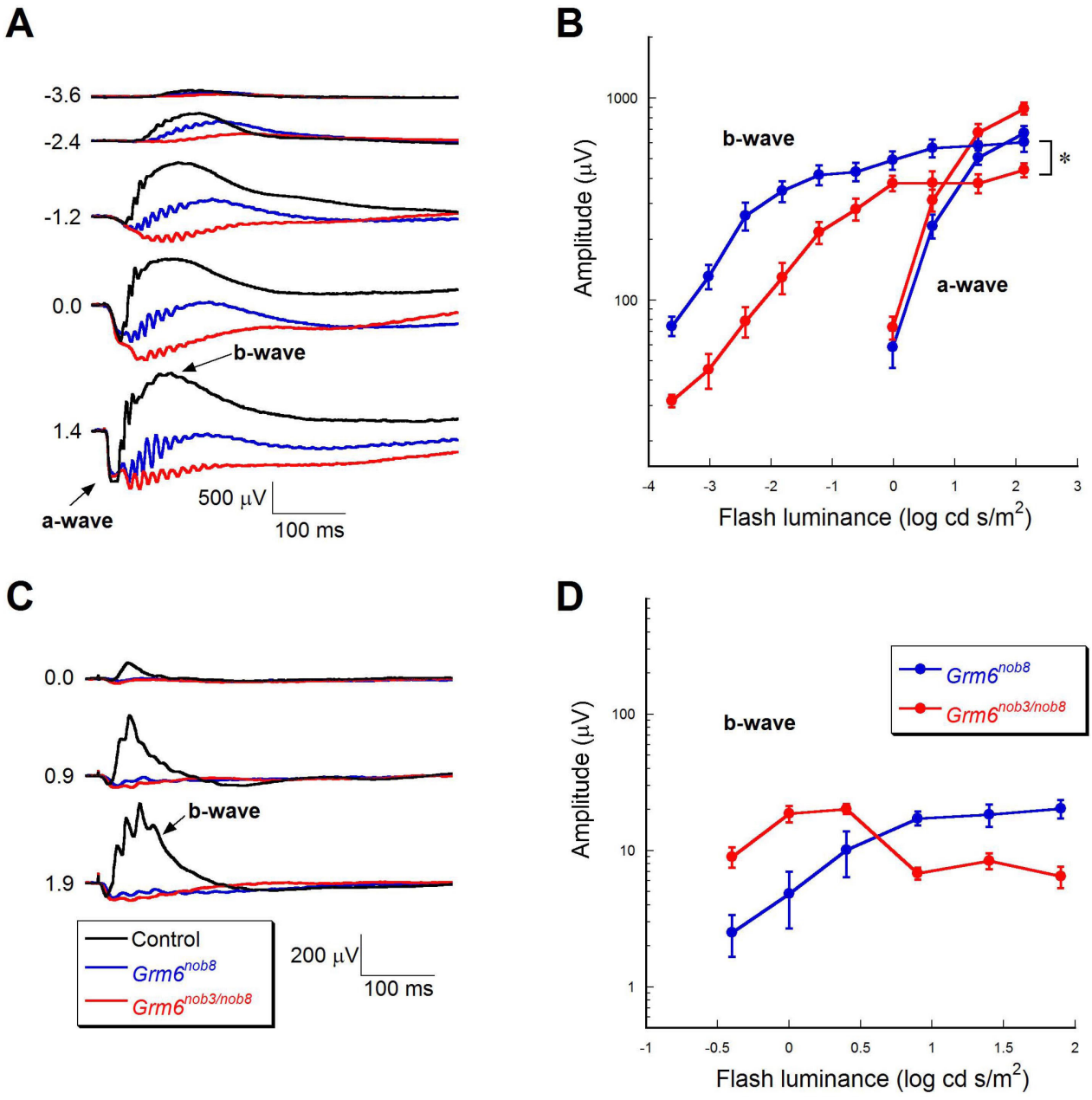

Figure 3. Comparison of ERGs from control, *Grm6*^{nob8}, and *Grm6*$^{nob3/nob8}$ mice at P28. ERGs were elicited under dark-adapted (**A**) or light-adapted (**C**) condition. Flash strength (in log cd s/m^2) is indicated on the left of each set of waveforms. **B**: Amplitude of dark-adapted a- and b-waves plotted as a function of flash luminance. **D**: Amplitude of light-adapted b-wave plotted as a function of flash luminance. In **B** and **D**, each plot indicates average +/− standard error of four (*Grm6*^{nob8}) or six (*Grm6*$^{nob3/nob8}$) mice. Repeated-measures ANOVA (ANOVA) was used to compare response functions. Compared to the *Grm6*^{nob8} mice, the *Grm6*$^{nob3/nob8}$ mice showed comparable a-wave ($p>0.05$) and reduced b-wave (*$p<0.01$) under the dark-adapted condition. The difference in the amplitude of the light-adapted b-wave was not statistically significant between groups ($p>0.05$).

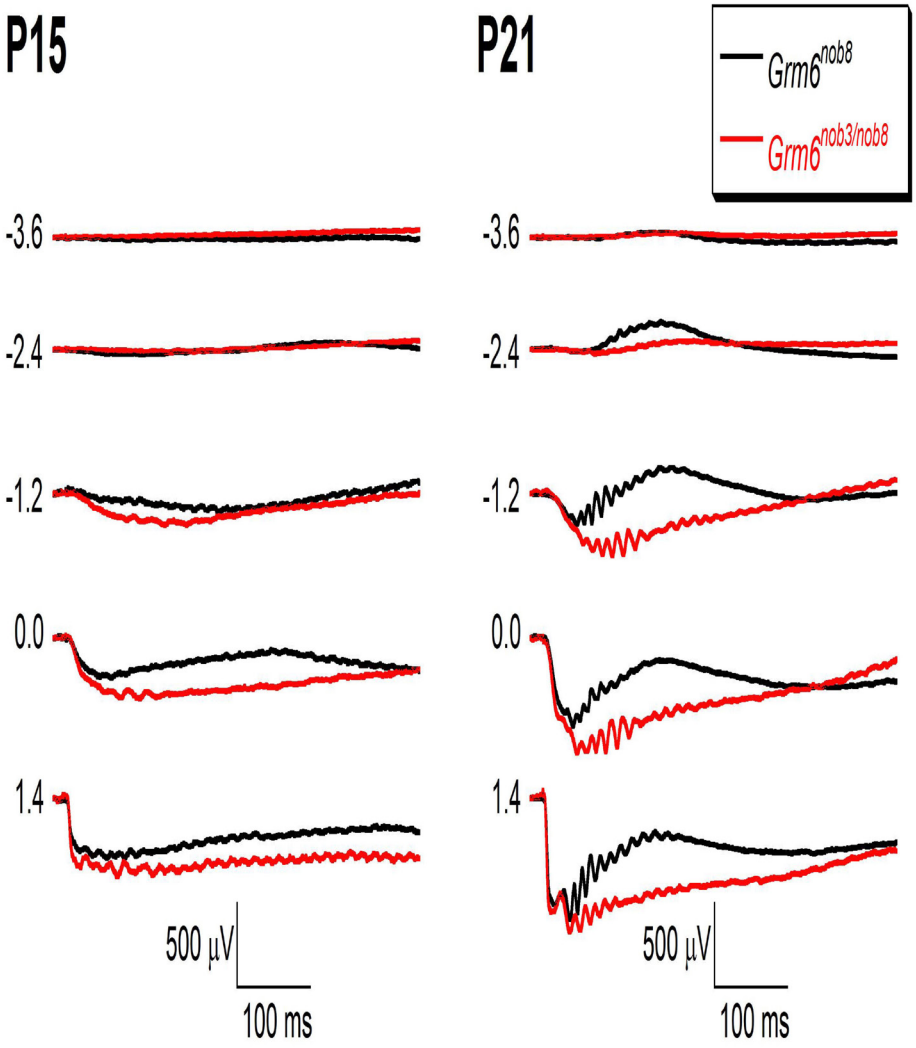

Figure 4. Comparison of dark-adapted ERG from *Grm6*^{nob8} and *Grm6*$^{nob3/nob8}$ mice at P15 and P21. Flash strength (in log cd s/m^2) is indicated on the left of each set of waveforms. At P15, no obvious b-wave was detected either from the *Grm6*^{nob8} or the *Grm6*$^{nob3/nob8}$ mice. At P21, a clear albeit reduced b-wave is present in all animals, with a greater reduction observed in the *Grm6*$^{nob3/nob8}$ mice when compared to the *Grm6*^{nob8} mice.

gene expression in the retina [31-33]. This has relevance for patients with cCSNB, as some are known to carry mutations that lie near the *nob8* locus [20], although we do not yet know if they also cause mislocalization. To test this hypothesis, we generated *Grm6*$^{nob3/nob8}$ compound heterozygotes, which express a single *Grm6*^{nob8} allele; *Grm6*^{nob3} is a null mutation [12]. In contrast to the possibility that mGluR6 protein and/or DBC function might be improved in the *Grm6*$^{nob3/nob8}$ retina compared to the *Grm6*^{nob8} retina, we observed neither normalization of mGluR6 localization nor an improved ERG b-wave. Instead, the b-wave was reduced in compound heterozygotes. These results indicate that simply reducing mutant mGluR6 protein will not provide a therapeutic avenue, and instead, suggest that some other means of improving mGluR6 trafficking to the DBC dendritic tips is needed.

A large number of mouse mutants have been reported where the ERG b-wave is reduced or abolished [34]. In general, the b-wave is abolished in mice with mutations in members of the DBC signaling cascade, including *Nyx* [35,36], *Trpm1* [30,37-39], *Gpr179* [40], *Lrit3* [41-43], *Gnb3* [44], *Gnb5* [45], *Gna01* [46], and *Grm6* [10-12], or in mice that lack DBCs [47]. In comparison, the b-wave is reduced but not abolished in mice with mutations in proteins that are involved in multiple other systems, including the control of glutamate release from photoreceptor terminals (*Cacna1f* [48-50], *Cacna2d4* [51,52], and *Cabp4* [53]), the development of retinal vasculature (*Fzd4* [54], *norrin* [55,56], and *Lrp5* [57]), or the dystroglycan complex (*pikachurin* [58], *POMGnT1* [59], and *Large* [60-62]). Based on the premise that the b-wave is abolished in mice with mutations of the DBC

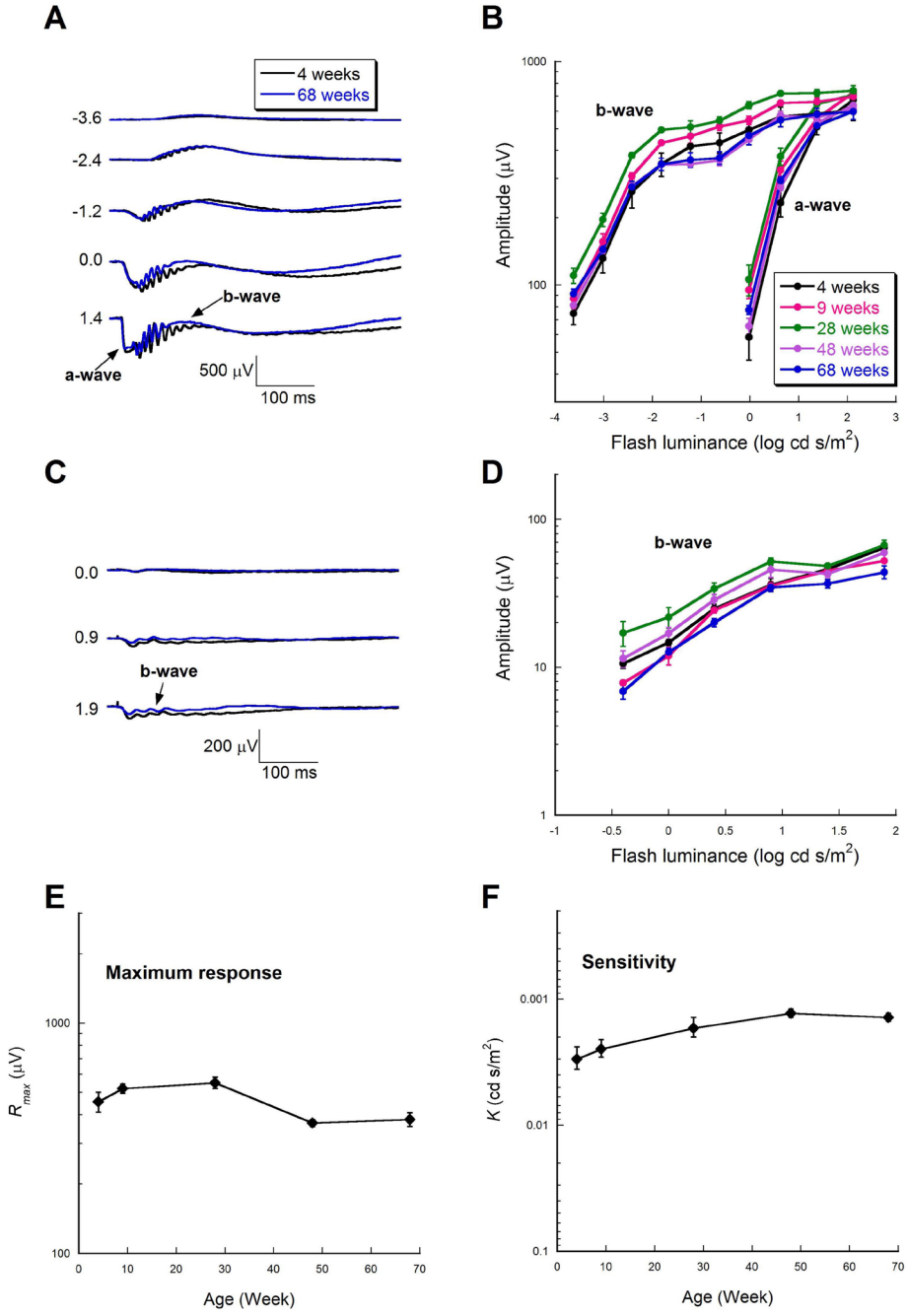

Figure 5. Longitudinal evaluation of ERG phenotype in adult *Grm6*^{nob8} mice. Comparison of dark- (**A**) and light-adapted (**C**) electroretinograms (ERGs) from young adult (4 weeks) and old (68 weeks) *Grm6*^{nob8} mice. Flash strength (in log cd s/m^2) is indicated on the left of each set of waveforms. **B**: Amplitude of dark-adapted a- and b-waves plotted as a function of flash luminance. **D**: Amplitude of the light-adapted b-wave plotted as a function of flash luminance. In **B** and **D**, each plot indicates average +/− standard error of four to five mice. Time course change in the maximum response (R_{max}, **E**) and sensitivity (K, **F**) parameters of the dark-adapted b-wave amplitude. When the R_{max} and K values of 4-week old mice were compared to those of older mice, the differences were not statistically significant (Aspin-Welch's t test, $p>0.05$).

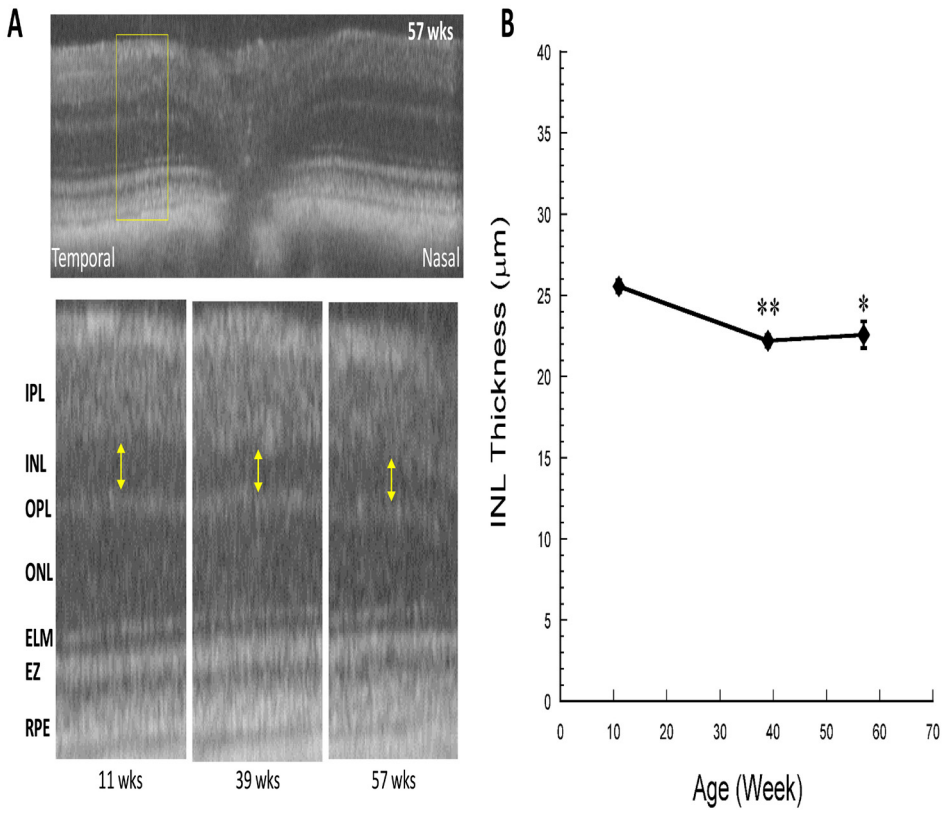

Figure 6. Longitudinal evaluation of SD-OCT image in adult *Grm6*^{nob8} mice. **A**: The upper image is a representative image taken across the horizontal meridian from a *Grm6*^{nob8} mouse at 57 weeks of age showing the well-defined laminar structure of the retina. Lower images were taken from *Grm6*^{nob8} mice at the ages indicated. ELM, external limiting membrane; EZ, ellipsoid zone; INL, inner nuclear layer; IPL, inner plexiform layer; ONL, outer nuclear layer; OPL, outer plexiform layer; RPE, retinal pigment epithelium. **B**: Thickness of the INL at 11, 39, and 57 weeks of age. The INL was thicker at 11 weeks of age, compared to the older ages (Aspin-Welch's *t* test; *p<0.05, **p<0.01). Each plot indicates average +/− standard error of four (11 weeks old) or three (39 and 57 weeks old) mice.

signaling process, we anticipated that the *nob8* mice would involve one of the processes that reduces but does not abolish DBC function [63], and were surprised when the mutation in *Grm6* was identified [14]. The *Grm6*^{nob8} mouse is the first mouse mutant to retain a b-wave in the presence of a mutation in a component of the DBC signaling cascade, and raises the possibility that similar variation may occur in human patients with CSNB, who are currently classified into complete and incomplete forms based in part on the absence of the b-wave in complete CSNB and on the presence of a reduced but not abolished b-wave in patients with incomplete CSNB [64]. Human patients expressing mutations in the glutamate ligand binding domain of GRM6, near the Met66 residue, have been reported [20]. It would be of interest to determine if they retained a measurable ERG b-wave compared to patients with CSNB with other *Grm6* mutations.

Protein-misfolding diseases, such as Alzheimer disease and Huntington's disease, involve the accumulation of misfolded proteins with abnormal conformation in neurons [65]. Furthermore, it has been reported that patients with complete CSNB harboring a *GRM6* mutation showed reduced inner retinal thickness with OCT imaging [66]. This motivated us to investigate whether long-term accumulation of mutant mGluR6 protein in DBC cell bodies might impact the inner retina of *Grm6*^{nob8} mice. ERG and SD-OCT analyses of *Grm6*^{nob8} mice at multiple ages indicate that rod DBC function is maintained at a reduced but stable level up to 68 weeks of age, and that a clear laminar structure of the retina is maintained up to 57 weeks old, with only a slight thinning of the INL. The absence of major age-related changes in the ERG b-wave or in the overall retinal structure indicated that DBCs tolerate the presence of mislocalized mutant p.Met66Leu mGluR6.

ACKNOWLEDGMENTS

This work was supported by the Foundation Fighting Blindness, and grants from the NIH (R01EY012354; R01EY019943; P30EY025585) and Research to Prevent Blindness (to Cleveland Clinic Cole Eye Institute and University of Louisville Department of Ophthalmology & Visual Sciences). NSP is a VA Research Career Scientist.

REFERENCES

1. Shiells RA, Falk G, Naghshineh S. Action of glutamate and aspartate analogues on rod horizontal and bipolar cells. Nature 1981; 294:592-4. [PMID: 6273752].
2. Slaughter MM, Miller RF. 2-amino-4-phosphonobutyric acid: a new pharmacological tool for retina research. Science 1981; 211:182-5. [PMID: 6255566].
3. Hood DC, Birch DG. Beta wave of the scotopic (rod) electroretinogram as a measure of the activity of human on-bipolar cells. J Opt Soc Am A Opt Image Sci Vis 1996; 13:623-33. [PMID: 8627419].
4. Kofuji P, Ceelen P, Zahs KR, Surbeck LW, Lester HA, Newman EA. Genetic inactivation of an inwardly rectifying potassium channel (Kir4.1 subunit) in mice: phenotypic impact in retina. J Neurosci 2000; 20:5733-40. [PMID: 10908613].
5. Robson JG, Frishman LJ. Response linearity and kinetics of the cat retina: the bipolar cell component of the dark-adapted electroretinogram. Vis Neurosci 1995; 12:837-50. [PMID: 8924408].
6. Robson JG, Frishman LJ. Photoreceptor and bipolar cell contributions to the cat electroretinogram: a kinetic model for the early part of the flash response. J Opt Soc Am A Opt Image Sci Vis 1996; 13:613-22. [PMID: 8627418].
7. Sharma S, Ball SL, Peachey NS. Pharmacological studies of the mouse cone electroretinogram. Vis Neurosci 2005; 22:631-6. [PMID: 16332274].
8. Dryja TP, McGee TL, Berson EL, Fishman GA, Sandberg MA, Alexander KR, Derlacki DJ, Rajagopalan AS. Night blindness and abnormal cone electroretinogram ON responses in patients with mutations in the GRM6 gene encoding mGluR6. Proc Natl Acad Sci USA 2005; 102:4884-9. [PMID: 15781871].
9. Zeitz C, van Genderen M, Neidhardt J, Luhmann UF, Hoeben F, Forster U, Wycisk K, Matyas G, Hoyng CB, Riemslag F, Meire F, Cremers FP, Berger W. Mutations in GRM6 cause autosomal recessive congenital stationary night blindness with a distinctive scotopic 15-Hz flicker electroretinogram. Invest Ophthalmol Vis Sci 2005; 46:4328-35. [PMID: 16249515].
10. Masu M, Iwakabe H, Tagawa Y, Miyoshi T, Yamashita M, Fukuda Y, Sasaki H, Hiroi K, Nakamura Y, Shigemoto R, Takada M, Nakamura K, Nakano K, Katsuki M, Nakanishi S. Specific deficit of the ON response in visual transmission by targeted disruption of the mGluR6 gene. Cell 1995; 80:757-65. [PMID: 7889569].
11. Pinto LH, Vitaterna MH, Shimomura K, Siepka SM, Balannik V, McDearmon EL, Omura C, Lumayag S, Invergo BM, Glawe B, Cantrell DR, Inayat S, Olvera MA, Vessey KA, McCall MA, Maddox D, Morgans CW, Young B, Pletcher MT, Mullins RF, Troy JB, Takahashi JS. Generation, identification and functional characterization of the nob4 mutation of Grm6 in the mouse. Vis Neurosci 2007; 24:111-23. [PMID: 17430614].
12. Maddox DM, Vessey KA, Yarbrough GL, Invergo BM, Cantrell DR, Inayat S, Balannik V, Hicks WL, Hawes NL, Byers S, Smith RS, Hurd R, Howell D, Gregg RG, Chang B, Naggert JK, Troy JB, Pinto LH, Nishina PM, McCall MA. Allelic variance between GRM6 mutants, Grm6nob3 and Grm6nob4 results in differences in retinal ganglion cell visual responses. J Physiol 2008; 586:4409-24. [PMID: 18687716].
13. Qian H, Ji R, Gregg RG, Peachey NS. Identification of a new mutant allele, Grm6(nob7), for complete congenital stationary night blindness. Vis Neurosci 2015; 32:E004-[PMID: 26241901].
14. Peachey NS, Hasan N, FitzMaurice B, Burrill S, Pangeni G, Karst SY, Reinholdt L, Berry ML, Strobel M, Gregg RG, McCall MA, Chang B. A Missense Mutation in Grm6 Reduces but Does Not Eliminate Mglur6 Expression or Rod Depolarizing Bipolar Cell Function. J Neurophysiol 2017; 845:118-[PMID: 28490646].
15. Free RB, Hazelwood LA, Cabrera DM, Spalding HN, Namkung Y, Rankin ML, Sibley DR. D1 and D2 dopamine receptor expression is regulated by direct interaction with the chaperone protein calnexin. J Biol Chem 2007; 282:21285-300. [PMID: 17395585].
16. Soto AG, Trejo J. N-linked glycosylation of protease-activated receptor-1 second extracellular loop: a critical determinant for ligand-induced receptor activation and internalization. J Biol Chem 2010; 285:18781-93. [PMID: 20368337].
17. Min C, Zheng M, Zhang X, Guo S, Kwon KJ, Shin CY, Kim HS, Cheon SH, Kim KM. N-linked Glycosylation on the N-terminus of the dopamine D2 and D3 receptors determines receptor association with specific microdomains in the plasma membrane. Biochim Biophys Acta 2015; 1853:41-51. [PMID: 25289757].
18. Igaz LM, Kwong LK, Lee EB, Chen-Plotkin A, Swanson E, Unger T, Malunda J, Xu Y, Winton MJ, Trojanowski JQ, Lee VM. Dysregulation of the ALS-associated gene TDP-43 leads to neuronal death and degeneration in mice. J Clin Invest 2011; 121:726-38. [PMID: 21206091].
19. Song D, Grieco S, Li Y, Hunter A, Chu S, Zhao L, Song Y, DeAngelis RA, Shi LY, Liu Q, Pierce EA, Nishina PM, Lambris JD, Dunaief JL. A murine RP1 missense mutation causes protein mislocalization and slowly progressive photoreceptor degeneration. Am J Pathol 2014; 184:2721-9. [PMID: 25088982].
20. Zeitz C, Robson AG, Audo I. Congenital stationary night blindness: an analysis and update of genotype-phenotype correlations and pathogenic mechanisms. Prog Retin Eye Res 2015; 45:58-110. [PMID: 25307992].
21. Hasan N, Ray TA, Gregg RG. CACNA1S expression in mouse retina: Novel isoforms and antibody cross-reactivity with GPR179. Vis Neurosci 2016; 33:E009-[PMID: 27471951].
22. Barthel LK, Raymond PA. Improved method for obtaining 3-microns cryosections for immunocytochemistry. J Histochem Cytochem 1990; 38:1383-8. [PMID: 2201738].

23. Cao Y, Pahlberg J, Sarria I, Kamasawa N, Sampath AP, Martemyanov KA. Regulators of G protein signaling RGS7 and RGS11 determine the onset of the light response in ON bipolar neurons. Proc Natl Acad Sci USA 2012; 109:7905-10. [PMID: 22547806].

24. Fulton AB, Rushton WA. The human rod ERG: correlation with psychophysical responses in light and dark adaptation. Vision Res 1978; 18:793-800. [PMID: 676087].

25. Bell BA, Kaul C, Hollyfield JG. A protective eye shield for prevention of media opacities during small animal ocular imaging. Exp Eye Res 2014; 127:280-7. [PMID: 25245081].

26. Bell BA, Kaul C, Bonilha VL, Rayborn ME, Shadrach K, Hollyfield JG. The BALB/c mouse: Effect of standard vivarium lighting on retinal pathology during aging. Exp Eye Res 2015; 135:192-205. [PMID: 25895728].

27. Thevenaz P, Ruttimann UE, Unser M. A pyramid approach to subpixel registration based on intensity. IEEE Trans Image Process 1998; 7:27-41. [PMID: 18267377].

28. Keeler CE, Sutcliffe E, Chaffee EL. A Description of the Ontogenetic Development of Retinal Action Currents in the House Mouse. Proc Natl Acad Sci USA 1928; 14:811-5. [PMID: 16587413].

29. Li C, Cheng M, Yang H, Peachey NS, Naash MI. Age-related changes in the mouse outer retina. Optom Vis Sci 2001; 78:425-30. [PMID: 11444632].

30. Peachey NS, Pearring JN, Bojang P Jr, Hirschtritt ME, Sturgill-Short G, Ray TA, Furukawa T, Koike C, Goldberg AF, Shen Y, McCall MA, Nawy S, Nishina PM, Gregg RG. Depolarizing bipolar cell dysfunction due to a Trpm1 point mutation. J Neurophysiol 2012; 108:2442-51. [PMID: 22896717].

31. LaVail MM, Yasumura D, Matthes MT, Drenser KA, Flannery JG, Lewin AS, Hauswirth WW. Ribozyme rescue of photoreceptor cells in P23H transgenic rats: long-term survival and late-stage therapy. Proc Natl Acad Sci USA 2000; 97:11488-93. [PMID: 11005848].

32. Liu J, Timmers AM, Lewin AS, Hauswirth WW. Ribozyme knockdown of the gamma-subunit of rod cGMP phosphodiesterase alters the ERG and retinal morphology in wild-type mice. Invest Ophthalmol Vis Sci 2005; 46:3836-44. [PMID: 16186371].

33. Yau EH, Butler MC, Sullivan JM. A cellular high-throughput screening approach for therapeutic trans-cleaving ribozymes and RNAi against arbitrary mRNA disease targets. Exp Eye Res 2016; 151:236-55. [PMID: 27233447].

34. Pardue MT, Peachey NS. Mouse b-wave mutants. Doc Ophthalmol 2014; 128:77-89. [PMID: 24395437].

35. Pardue MT, McCall MA, LaVail MM, Gregg RG, Peachey NS. A naturally occurring mouse model of X-linked congenital stationary night blindness. Invest Ophthalmol Vis Sci 1998; 39:2443-9. [PMID: 9804152].

36. Gregg RG, Kamermans M, Klooster J, Lukasiewicz PD, Peachey NS, Vessey KA, McCall MA. Nyctalopin expression in retinal bipolar cells restores visual function in a mouse model of complete X-linked congenital stationary night blindness. J Neurophysiol 2007; 98:3023-33. [PMID: 17881478].

37. Morgans CW, Zhang J, Jeffrey BG, Nelson SM, Burke NS, Duvoisin RM, Brown RL. TRPM1 is required for the depolarizing light response in retinal ON-bipolar cells. Proc Natl Acad Sci USA 2009; 106:19174-8. [PMID: 19861548].

38. Shen Y, Heimel JA, Kamermans M, Peachey NS, Gregg RG, Nawy S. A transient receptor potential-like channel mediates synaptic transmission in rod bipolar cells. J Neurosci 2009; 29:6088-93. [PMID: 19439586].

39. Koike C, Obara T, Uriu Y, Numata T, Sanuki R, Miyata K, Koyasu T, Ueno S, Funabiki K, Tani A, Ueda H, Kondo M, Mori Y, Tachibana M, Furukawa T. TRPM1 is a component of the retinal ON bipolar cell transduction channel in the mGluR6 cascade. Proc Natl Acad Sci USA 2010; 107:332-7. [PMID: 19966281].

40. Peachey NS, Ray TA, Florijn R, Rowe LB, Sjoerdsma T, Contreras-Alcantara S, Baba K, Tosini G, Pozdeyev N, Iuvone PM, Bojang P Jr, Pearring JN, Simonsz HJ, van Genderen M, Birch DG, Traboulsi EI, Dorfman A, Lopez I, Ren H, Goldberg AF, Nishina PM, Lachapelle P, McCall MA, Koenekoop RK, Bergen AA, Kamermans M, Gregg RG. GPR179 is required for depolarizing bipolar cell function and is mutated in autosomal-recessive complete congenital stationary night blindness. Am J Hum Genet 2012; 90:331-9. [PMID: 22325362].

41. Neuille M, El Shamieh S, Orhan E, Michiels C, Antonio A, Lancelot ME, Condroyer C, Bujakowska K, Poch O, Sahel JA, Audo I, Zeitz C. Lrit3 deficient mouse (nob6): a novel model of complete congenital stationary night blindness (cCSNB). PLoS One 2014; 9:e90342-[PMID: 24598786].

42. Charette JR, Samuels IS, Yu M, Stone L, Hicks W, Shi LY, Krebs MP, Naggert JK, Nishina PM, Peachey NS. A Chemical Mutagenesis Screen Identifies Mouse Models with ERG Defects. Adv Exp Med Biol 2016; 854:177-83. [PMID: 26427409].

43. Hasan N, Pangeni G, Cobb CA, Ray TA, Nettesheim ER, Ertel KJ, Lipinski DM, McCall MA, Gregg RG. Presynaptic Expression of LRIT3 Transsynaptically Organizes the Postsynaptic Glutamate Signaling Complex Containing TRPM1. Cell Reports 2019; 27:3107-16.e3. [PMID: 31189098].

44. Dhingra A, Ramakrishnan H, Neinstein A, Fina ME, Xu Y, Li J, Chung DC, Lyubarsky A, Vardi N. Gbeta3 is required for normal light ON responses and synaptic maintenance. J Neurosci 2012; 32:11343-55. [PMID: 22895717].

45. Rao A, Dallman R, Henderson S, Chen CK. Gbeta5 is required for normal light responses and morphology of retinal ON-bipolar cells. J Neurosci 2007; 27:14199-204. [PMID: 18094259].

46. Dhingra A, Lyubarsky A, Jiang M, Pugh EN Jr, Birnbaumer L, Sterling P, Vardi N. The light response of ON bipolar neurons requires G[alpha]o. J Neurosci 2000; 20:9053-8. [PMID: 11124982].

47. Peachey NS, Quiambao AB, Xu X, Pardue MT, Roveri L, McCall MA, Al-Ubaidi MR. Loss of bipolar cells resulting

from the expression of bcl-2 directed by the IRBP promoter. Exp Eye Res 2003; 77:477-83. [PMID: 12957146].

48. Ball SL, Powers PA, Shin HS, Morgans CW, Peachey NS, Gregg RG. Role of the beta(2) subunit of voltage-dependent calcium channels in the retinal outer plexiform layer. Invest Ophthalmol Vis Sci 2002; 43:1595-603. [PMID: 11980879].

49. Mansergh F, Orton NC, Vessey JP, Lalonde MR, Stell WK, Tremblay F, Barnes S, Rancourt DE, Bech-Hansen NT. Mutation of the calcium channel gene Cacna1f disrupts calcium signaling, synaptic transmission and cellular organization in mouse retina. Hum Mol Genet 2005; 14:3035-46. [PMID: 16155113].

50. Knoflach D, Kerov V, Sartori SB, Obermair GJ, Schmuckermair C, Liu X, Sothilingam V, Garcia Garrido M, Baker SA, Glosmann M, Schicker K, Seeliger M, Lee A, Koschak A. Cav1.4 IT mouse as model for vision impairment in human congenital stationary night blindness type 2. Channels (Austin) 2013; 7:503-13. [PMID: 24051672].

51. Ruether K, Grosse J, Matthiessen E, Hoffmann K, Hartmann C. Abnormalities of the photoreceptor-bipolar cell synapse in a substrain of C57BL/10 mice. Invest Ophthalmol Vis Sci 2000; 41:4039-47. [PMID: 11053310].

52. Wycisk KA, Budde B, Feil S, Skosyrski S, Buzzi F, Neidhardt J, Glaus E, Nurnberg P, Ruether K, Berger W. Structural and functional abnormalities of retinal ribbon synapses due to Cacna2d4 mutation. Invest Ophthalmol Vis Sci 2006; 47:3523-30. [PMID: 16877424].

53. Haeseleer F, Imanishi Y, Maeda T, Possin DE, Maeda A, Lee A, Rieke F, Palczewski K. Essential role of Ca2+-binding protein 4, a Cav1.4 channel regulator, in photoreceptor synaptic function. Nat Neurosci 2004; 7:1079-87. [PMID: 15452577].

54. Ye X, Wang Y, Cahill H, Yu M, Badea TC, Smallwood PM, Peachey NS, Nathans J. Norrin, frizzled-4, and Lrp5 signaling in endothelial cells controls a genetic program for retinal vascularization. Cell 2009; 139:285-98. [PMID: 19837032].

55. Berger W, van de Pol D, Bachner D, Oerlemans F, Winkens H, Hameister H, Wieringa B, Hendriks W, Ropers HH. An animal model for Norrie disease (ND): gene targeting of the mouse ND gene. Hum Mol Genet 1996; 5:51-9. [PMID: 8789439].

56. Ruether K, van de Pol D, Jaissle G, Berger W, Tornow RP, Zrenner E. Retinoschisislike alterations in the mouse eye caused by gene targeting of the Norrie disease gene. Invest Ophthalmol Vis Sci 1997; 38:710-8. [PMID: 9071226].

57. Charette JR, Earp SE, Bell BA, Ackert-Bicknell CL, Godfrey DA, Rao S, Anand-Apte B, Nishina PM, Peachey NS. A mutagenesis-derived Lrp5 mouse mutant with abnormal retinal vasculature and low bone mineral density. Mol Vis 2017; 23:140-8. [PMID: 28356706].

58. Sato S, Omori Y, Katoh K, Kondo M, Kanagawa M, Miyata K, Funabiki K, Koyasu T, Kajimura N, Miyoshi T, Sawai H, Kobayashi K, Tani A, Toda T, Usukura J, Tano Y, Fujikado T, Furukawa T. Pikachurin, a dystroglycan ligand, is essential for photoreceptor ribbon synapse formation. Nat Neurosci 2008; 11:923-31. [PMID: 18641643].

59. Liu J, Ball SL, Yang Y, Mei P, Zhang L, Shi H, Kaminski HJ, Lemmon VP, Hu H. A genetic model for muscle-eye-brain disease in mice lacking protein O-mannose 1,2-N-acetylglucosaminyltransferase (POMGnT1). Mech Dev 2006; 123:228-40. [PMID: 16458488].

60. Holzfeind PJ, Grewal PK, Reitsamer HA, Kechvar J, Lassmann H, Hoeger H, Hewitt JE, Bittner RE. Skeletal, cardiac and tongue muscle pathology, defective retinal transmission, and neuronal migration defects in the Large(myd) mouse defines a natural model for glycosylation-deficient muscle - eye - brain disorders. Hum Mol Genet 2002; 11:2673-87. [PMID: 12354792].

61. Lee Y, Kameya S, Cox GA, Hsu J, Hicks W, Maddatu TP, Smith RS, Naggert JK, Peachey NS, Nishina PM. Ocular abnormalities in Large(myd) and Large(vls) mice, spontaneous models for muscle, eye, and brain diseases. Mol Cell Neurosci 2005; 30:160-72. [PMID: 16111892].

62. Peachey NS, Sturgill-Short GM. Response properties of slow PIII in the Large (vls) mutant. Doc Ophthalmol 2012; 125:203-9. [PMID: 22865473].

63. Xue Y, Shen SQ, Corbo JC, Kefalov VJ. Circadian and light-driven regulation of rod dark adaptation. Sci Rep 2015; 5:17616-[PMID: 26626567].

64. Miyake Y, Yagasaki K, Horiguchi M, Kawase Y, Kanda T. Congenital stationary night blindness with negative electroretinogram. A new classification. Arch Ophthalmol 1986; 104:1013-20. [PMID: 3488053].

65. Remondelli P, Renna M. The Endoplasmic Reticulum Unfolded Protein Response in Neurodegenerative Disorders and Its Potential Therapeutic Significance. Front Mol Neurosci 2017; 10:187-[PMID: 28670265].

66. Godara P, Cooper RF, Sergouniotis PI, Diederichs MA, Streb MR, Genead MA, McAnany JJ, Webster AR, Moore AT, Dubis AM, Neitz M, Dubra A, Stone EM, Fishman GA, Han DP, Michaelides M, Carroll J. Assessing retinal structure in complete congenital stationary night blindness and Oguchi disease. Am J Ophthalmol 2012; 154:987-1001.e1. [PMID: 22959359].

Articles are provided courtesy of Emory University and the Zhongshan Ophthalmic Center, Sun Yat-sen University, P.R. China. The print version of this article was created on 31 December 2019. This reflects all typographical corrections and errata to the article through that date. Details of any changes may be found in the online version of the article.